

Accepted Manuscript

Overcoming resistance to cisplatin by inhibition of glutathione S-transferases (GSTs) with ethacraplatin micelles *in vitro* and *in vivo*

Shuyi Li, Chan Li, Shubin Jin, Juan Liu, Xiangdong Xue, Ahmed Shaker Eltahan, Jiadong Sun, Jingjie Tan, Jinchen Dong, Xing-Jie Liang



PII: S0142-9612(17)30531-8

DOI: [10.1016/j.biomaterials.2017.08.021](https://doi.org/10.1016/j.biomaterials.2017.08.021)

Reference: JBMT 18222

To appear in: *Biomaterials*

Received Date: 6 April 2017

Revised Date: 9 July 2017

Accepted Date: 14 August 2017

Please cite this article as: Li S, Li C, Jin S, Liu J, Xue X, Eltahan AS, Sun J, Tan J, Dong J, Liang X-J, Overcoming resistance to cisplatin by inhibition of glutathione S-transferases (GSTs) with ethacraplatin micelles *in vitro* and *in vivo*, *Biomaterials* (2017), doi: 10.1016/j.biomaterials.2017.08.021.

This is a PDF file of an unedited manuscript that has been accepted for publication. As a service to our customers we are providing this early version of the manuscript. The manuscript will undergo copyediting, typesetting, and review of the resulting proof before it is published in its final form. Please note that during the production process errors may be discovered which could affect the content, and all legal disclaimers that apply to the journal pertain.

Overcoming resistance to cisplatin by inhibition of glutathione S-transferases (GSTs) with ethacraplatin micelles *in vitro* and *in vivo*

Shuyi Li^{a,b,1}, Chan Li^{*a,b,1}, Shubin Jin^c, Juan Liu^d, Xiangdong Xue^a, Ahmed Shaker Eltahan^{a,b}, Jiadong Sun^a, Jingjie Tan^a, Jinchen Dong^a and Xing-Jie Liang^{*,a,b}

^a Laboratory of Controllable Nanopharmaceuticals, Chinese Academy of Sciences (CAS) Center for Excellence in Nanoscience; and CAS Key Laboratory for Biomedical Effects of Nanomaterials and Nanosafety, National Center for Nanoscience and Technology of China, No.11, First North Road, Zhongguancun, Beijing, 100190, P. R. China.

^b University of Chinese Academy of Sciences, Beijing 100049, P. R. China

^c Beijing Municipal Institute of Labour Protection, No.55 Taoranting Road, Xicheng District, Beijing, 100054, P. R. China.

^d Tissue Engineering Lab, Beijing Institute of Transfusion Medicine, Beijing 1000850, P. R. China.

¹S.L. and C.L. contributed equally to this work.

*Corresponding author:

Xing-Jie Liang, Tel: +86-010-82545569; Fax: +86-010-62656765; Email: liangxj@nanoctr.cn;

Chan Li, Tel: +86-010-82545615; Fax: +86-010-62656765; Email: lic@nanoctr.cn.

Abstract

Platinum-based DNA-adducting agents are used extensively in the clinic for cancer chemotherapy. However, the anti-tumor efficacy of these drugs is severely limited by cisplatin resistance, and this can lead to the failure of chemotherapy. One of cisplatin resistance mechanisms is associated with overexpression of glutathione S-transferases (GSTs), which would accelerate the deactivation of cisplatin and decrease its antitumor efficiency. Nanoscale micelles encapsulating ethacraplatin, a conjugate of cisplatin and ethacrynic acid (an effective GSTs inhibitor), can enhance the accumulation of active cisplatin in cancer cells by inhibiting the activity of GSTs and circumventing deactivation of cisplatin. *In vitro* and *in vivo* results provide strong evidence that GSTs inhibitor-modified cisplatin prodrug combined with nanoparticle encapsulation favor high effective platinum accumulation, significantly enhanced antitumor efficacy against cisplatin-resistant cancer and decreased system toxicity. It is believed that these ethacraplatin-loaded micelles have the ability of overcoming resistance of cancers toward cisplatin and will improve the prospects for chemotherapy of cisplatin-resistant cancers in the near future.

cisplatin resistance | glutathione S-transferases (GSTs) | ethacraplatin | drug delivery

1. Introduction

Cancer endangers the health of humans around the world [1]. Chemotherapy is one of the leading choices for cancer treatment. Three platinum-based DNA-adducting agents, cisplatin, carboplatin, and oxaliplatin, are most widely used in standard-of-care chemotherapy for many types of cancer. However, in the clinic, platinum-based

agents only show excellent efficacy in the early stage of chemotherapy, and their effectiveness subsequently becomes weakened by the development of cisplatin resistance. Thus, cisplatin resistance is a key factor leading to chemotherapy failure. In some types of cancer, the mechanism of cisplatin resistance is mainly associated with the intracellular overexpression of glutathione S-transferases (GSTs) [2, 3].

GSTs are crucial detoxification enzymes that are capable of catalyzing the conjugation of glutathione (GSH) with a multitude of xenobiotics, one of which is cisplatin. Cisplatin undergoes detoxification by GSH more readily in resistant cells due to the overexpression of GSTs. Hence, GSTs have been regarded as promising drug targets to reverse cisplatin resistance in cancers. Especially, it has been reported that the expression of GST- π is positively correlated with cisplatin resistance of tumors.[2, 3] Subsequently, some strategies have been successfully developed to inhibit their activity [4-6].

One smart approach is to suppress intratumoral GST activity by designing bifunctional Pt(IV) prodrugs that have greater stability and are activated locally. This allows for enhanced accumulation of active platinum(II) at the target sites. In addition, Pt(IV) prodrugs generally exhibit improved properties such as lipophilicity and active targeting as a result of modification of the axial ligands. More importantly, Pt(IV) prodrugs with dual-threat capabilities, such as mitaplatin and Pt(IV)(α -TOS)(OEt), provide a more effective therapeutic option because they can target mitochondria and genomic DNA simultaneously [7-9].

Ethacraplatin (EA-Pt) is a bifunctional Pt(IV) prodrug that releases its ethacrynic acid (EA) moiety, an effective GSTs inhibitor, and active platinum(II) metal center by

reduction in cancer cells. It can potently inhibit GSTs, thereby enhancing accumulation of active cytotoxic Pt(II) in the cancer cell, which facilitates generation of platinum-DNA adducts, and consequently reverses drug resistance. This suggests that ethacraplatin possesses a great potential for therapy of cisplatin-resistant cancer. However, ethacraplatin is a hydrophobic molecule with poor water solubility. A previous study showed that ethacraplatin had no better long-term (>24 h) anticancer efficacy *in vitro* than cisplatin, which may impede its further application *in vivo* [10]. It is imperative to find an approach to overcome these limitations. Nanotechnology has developed rapidly in the past two decades, and has displayed tremendous promise for developing cancer therapies. Various drug delivery systems have been explored which have opened up new prospects for altering the properties of drugs, alleviating their systemic cytotoxicity and enhancing their anti-cancer efficacy *in vitro* and *in vivo* [11-20]. Lippard and colleagues encapsulated mitaplatin into nanoparticles for cancer therapy [21]. Their results demonstrated that this nanoparticle formation strategy was beneficial in reducing the side effects of mitaplatin by decreasing unwanted accumulation of platinum in the kidneys. In addition, encapsulation of mitaplatin in nanoparticles did not compromise the long-term chemotherapeutic effect. Lin and coworkers developed a self-assembly delivery system with pegylated Zn pyrophosphate nanoscale coordination polymers (NCPs), which are capable of carrying cisplatin or oxaliplatin prodrugs with high levels of drug loading [22]. Data from a multitude of *in vivo* experiments indicated that these two novel drug delivery systems are advantageous over free drugs in biodistribution and therapeutic efficacy. Some nanoparticles physically loading cisplatin were also developed [23]. Duan *et al* fabricated cisplatin-loaded EGF modified mPEG-PLGA-PLL nanoparticles [24], which can improve antitumor efficiency for SKOV3 cancer *in vitro* and *in vivo*, and reduce nephrotoxicity and systemic toxicity. Alexiou *et al* utilized superparamagnetic iron oxide nanoparticles (SPIONs) with a dextran and hyaluronic acid (HA) coating to deliver cisplatin [25]. The developed carrier reserved superparamagnetic property and possessed high biocompatibility. The cisplatin-loaded nanoparticle showed comparable antitumor activity to cisplatin. This work represents a promising

application of magnetic drug targeting for cancer therapy. They have potential for further translation in the clinic in the future.

Here we employed an FDA-approved adjuvant, 1,2-distearoyl-sn-glycero-3-phosphoethanolamine-N-[methoxy(polyethylene glycol)-2000] (DSPE-PEG₂₀₀₀), to form micelles and deliver ethacraplatin (EA-Pt). The ethacraplatin-containing micelles (M-EA-Pt) were demonstrated to improve the poor water-solubility of free ethacraplatin, increase the drug content at the tumor site by the enhanced permeability and retention (EPR) effect, and improve the antitumor activity without increasing system toxicity in cisplatin-resistant cancer models *in vitro* and *in vivo*.

2. Materials and Methods

2.1. Materials

Cisplatin was purchased from Sigma-Aldrich Company (St. Louis, MO). Ethacrynic acid was purchased from Enzo Life Sciences Inc (NY, USA). 1,2-distearoyl-sn-glycero-3-phosphoethanolamine-N-[methoxy(polyethylene glycol)-2000] (DSPE-PEG₂₀₀₀) was purchased from Lipoid GmbH (Ludwigshafen, Germany). Coumarin 6 was purchased from J&K Scientific Ltd (Beijing, China). Methanol was purchased from Avantor Performance Materials Inc (PA, USA).

2.2. Synthesis and characterization of ethacraplatin

Ethacraplatin was synthesized according to the literature. Briefly, *cis, cis, trans*-Pt(NH₃)₂Cl₂(OH)₂ was first synthesized. Cisplatin (500 mg) was added to water (10 mL) to form a suspension, then 30% hydrogen peroxide (4 mL) was added and stirred at 50 °C. After 1 h, the suspension was stored at 4 °C overnight. The precipitated solid

$\text{Pt}(\text{NH}_3)_2\text{Cl}_2(\text{OH})_2$ was filtered off and washed with cold water and ethanol. Light yellow crystals of $\text{Pt}(\text{NH}_3)_2\text{Cl}_2(\text{OH})_2$ were obtained. Next, excess oxalyl chloride (2.5 mL) was mixed with ethacrynic acid (500 mg) and refluxed at 70 °C for 60 min. Unreacted oxalyl chloride was removed under vacuum. In order to remove the oxalyl chloride completely, dry THF (2×5 mL) was added and removed by vacuum extraction. When the extraction procedure was complete, ethacrynic acid chloride remained as a pale yellow oil-like compound. The obtained ethacrynic acid chloride was mixed with $\text{Pt}(\text{NH}_3)_2\text{Cl}_2(\text{OH})_2$ (116 mg) in dry THF (5 mL) and stirred at 70 °C. After approximately 40 min, THF was removed under vacuum. Acetone (5 mL) was then added, followed by water (25 mL), and the mixture was stored at 4 °C overnight. After removal of the acetone under vacuum, the water was discarded. The residue was washed twice with water, then dried at 60 °C. The solid left was resuspended in excess diethyl ether and filtered. The final product EA-Pt is an off-white solid.

Molar masses and molar mass distributions of EA-Pt were determined on a Bruker Amazon SL electrospray ionization mass spectrometer (ESI-MS). Nuclear magnetic resonance (NMR) spectra were registered on a Bruker AVANCE III NMR spectrometer. Ultraviolet spectra (UV-Vis) were recorded on a LabTech Bluestar A ultraviolet spectrometer (LabTech, China). The purity analysis of EA-Pt was carried out by high-performance liquid chromatography (HPLC, LC-20A, Shimadzu). EA-Pt was analyzed on an Eclipse XDB-C18 analytical column (250 mm \times 4.6 mm, 5 μm , Agilent). The gradient was varied from 85% to 95% methanol (the water fraction varied from 15% to 5% accordingly). The flow rate was 1.5 mL/min at 40 °C, and the

gradient procedure lasted for 20 min. The UV-Vis detector was set at the wavelength of 275 nm.

2.3. Preparation of ethacraplatin-loaded nanomicelles

Ethacraplatin-loaded micelles (M-EA-Pt) were synthesized from DSPE-PEG₂₀₀₀ and ethacraplatin by the film dispersion method. Ethacraplatin and DSPE-PEG₂₀₀₀ (1:7, w/w) were dispersed in 5 mL methanol. After removing the solvent by vacuum rotary evaporation, a dry film was formed, which was then hydrated with deionized water at room temperature for 10 min. Coumarin 6-loaded nanomicelles were prepared according to the method described above. The morphology of the micelles was measured by electron microscopy. The hydrated diameter of the micelles was detected by dynamic light scattering (DLS) using a Zetasizer 5000 (Malvern Instruments, Malvern, Worcestershire, UK). After formation of M-EA-Pt, the free drug that was not encapsulated into the micelles was removed by filtration using 0.22 μm membrane. The quantity of ethacraplatin in the M-EA-Pt was determined using NexION 300X inductively coupled plasma mass spectroscopy (ICP-MS, PerkinElmer, USA). The encapsulation efficiency (EE) and drug loading efficiency (DLE) were determined using the formulas below:

$$\text{Encapsulation efficiency (\%)} = \frac{\text{weight of loaded EA-Pt}}{\text{weight of EA-Pt in feed}} \times 100\%$$

$$\text{Drug loading efficiency (\%)} = \frac{\text{weight of loaded EA-Pt}}{\text{weight of EA-Pt-loaded micelles}} \times 100\%$$

2.4. Ethacraplatin release from micelles

The release profile of M-EA-Pt was detected by dialysis using minidialysis tubes with a molecular mass cut off of 6 kDa - 8 kDa (Millipore, USA). A suspension of M-EA-Pt in water was divided equally (100 μ L) into multiple minidialysis tubes. All these minidialysis tubes were soaked in a same beaker containing 2 L PBS (pH 7.4) and stirred in the dark at 37 $^{\circ}$ C. After 0, 1, 4, 6, 16, 25, 48, 72, 96, 120 and 144 h, one minidialysis tube was withdrawn. The micellular suspension remained in each minidialysis tube was transferred and the platinum content was quantified by ICP-MS after digestion using aqua regia. The percentage of EA-Pt released at different time (P_x) is calculated as follows: $P_x = (Pt_0 - Pt_x) / Pt_0 \times 100\%$, Pt_0 is the initial platinum content added in the tube, and Pt_x is the platinum content remained in the tube at different time. All experiments were carried out in triplicate.

2.5. Cell culture

The parent cell line BEL7404 and its cisplatin-resistant derivative BEL 7404-CP20 were presented as gifts by Michael M. Gottesman's laboratory at NCI, NIH. BEL7404-CP20 cells were cultured in medium including 5 μ g/mL cisplatin. Both cell lines were both cultured in an atmosphere containing 5% CO₂ at 37 $^{\circ}$ C using DMEM-high glucose (Wisent, Canada) with 10% fetal bovine serum (Wisent, Canada), 100 units/mL penicillin, and 100 μ g/mL streptomycin (Gibico, Invitrogen). For *in vitro* experiments, ethacraplatin was pre-dissolved in ethanol and further diluted with DMEM-high glucose to the required concentration. Cisplatin and M-EA-Pt were pre-dissolved in PBS and further diluted with fresh medium to the same concentration. For *in vivo* experiments, ethacraplatin was pre-dissolved in ethanol and further diluted

with saline to the required concentration. Cisplatin and M-EA-Pt were dissolved in saline.

2.6. *GST- π Expression*

Expression of GST- π was detected by immunofluorescence. BEL7404 or BEL7404-CP20 cells were fixed with 4% cold paraformaldehyde for 15 min. The cells were blocked for 1 h in 1% BSA PBS and then incubated with monoclonal antibody against GST- π (1:100, Abcam, Cambridge, UK) overnight. The membrane was washed with PBS and then incubated for 1 h with goat anti-mouse secondary antibody conjugated with FITC (1:1000, zsBio, Beijing, China). The nuclei were stained with DAPI (10 μ g/mL, Invitrogen, USA) for 1 min after washing three times with PBS. Cells were visualized with a confocal laser-scanning microscope (LSM710, Carl Zeiss) with excitation at 405 nm for DAPI and 488 nm for FITC. Cells that were incubated with secondary antibody only were regarded as the control.

Expression of GST- π in BEL7404 or BEL7404-CP20 cells was also determined by western blotting. Cells were dissolved in RIPA buffer containing protease inhibitor cocktail (cOmplete, Roche, Switzerland) to obtain proteins. After centrifugation, Cell lysates were collected after centrifugation. Then, protein concentration was determined by BCA Protein Assay kit (Thermo Fisher, USA). Proteins were separated by electrophoresis using 10% SDS-PAGE gel and then transferred onto PVDF membrane. Membranes were exposed to monoclonal antibody against GST- π (1:200, Abcam, Cambridge, UK) overnight at 4 °C. After washing, membranes were treated with horseradish peroxidase (HRP)-conjugated secondary antibody (1:5000, zsBio,

Beijing, China) for 1 hour at room temperature and detected by chemiluminescence imaging system (ChemiDoc Touch , Biorad, USA). β -actin was used as a protein-loading control.

2.7. *GST activity*

BEL7404 and BEL7404-CP20 cancer cells (1.5×10^5) were seeded in 35 mm² dishes and further cultured for 24 h. Then, the cells were harvested using a rubber policeman and centrifuged at 1000 rpm. The cell pellets were resuspended in 30 μ L cold buffer (100 mM potassium phosphate, pH 7.0, including 2 mM EDTA) containing protease inhibitor. The whole cells were lysed by freezing and thawing, and centrifuged at 10000 g for 15 min at 4 °C. The supernatant was removed for assay. The GST activity was detected using a Glutathione-S-Transferase (GST) Assay Kit (Sigma-Aldrich, USA) and the protein content was measured using a BCA Protein Assay Kit (Thermo Fisher, USA). All experiments were carried out in triplicate.

2.8. *Inhibition of GST activity in vitro*

BEL7404-CP20 cells (1.5×10^5) were seeded in 35 mm² dishes and further cultured for 24 h. After that, the cells were treated with fresh medium containing cisplatin, ethacraplatin or M-EA-Pt at platinum concentrations of 50 μ M. After 4 h, the cells were harvested and treated as described in the previous paragraph. Finally, the supernatant was used to determine the residual GST activity. Untreated cells in culture medium were used as the control. All experiments were carried out in triplicate.

2.9. Internalization and distribution of micelles *in vitro*

Firstly, a fluorescent molecule coumarin 6 (C6) was encapsulated into DSPE-PEG₂₀₀₀ micelles to monitor the cellular uptake of the micelles. Next, BEL7404 cells or BEL7404-CP20 cells were seeded in 35 mm² dishes (10⁵ cells per dish) and cultured in DMEM-high glucose medium. After 48 h, the cells were exposed to 0.5 µg/mL free C6 or C6 Micelles (M-C6) in culture medium. After incubation for 30 min, the cells were rinsed repeatedly with PBS. The acidic organelles were then stained with LysoTracker® Deep Red (1:1000, Eugene, Oregon, USA) for 15 min. After three washes with PBS, the cell nuclei were stained with Hoechst 33342 (10 µg/mL, Sigma, USA) for 15 min. Thereafter, the live cells were imaged by confocal microscopy (LSM710, Carl Zeiss) with excitation at 405 nm for Hoechst 33342, 488 nm for coumarin 6 and 633 nm for LysoTracker® Deep Red. Statistical analysis data of the mean fluorescence intensity of C6 was obtained by Image J software.

2.10. Analysis of platinum-DNA adduct formation

BEL 7404-CP 20 cells were grown at a concentration of 10⁷ cells in 100 mm² dishes for 24 h. Then cells were incubated with fresh medium containing PBS, cisplatin, free EA-Pt, or M-EA-Pt at platinum concentrations of 50 µM. After 4 h, the cells were rinsed 3 times with PBS, trypsinized, and centrifuged for 3 min at 1000 g. The genomic DNA was extracted using a GenElute Mammalian Genomic DNA Miniprep Kit. The DNA concentration was determined by UV-visible spectroscopy.

After digestion, the platinum content was quantified by ICP-MS. All experiments were carried out in triplicate.

2.11. *In vitro* antitumor activity

BEL7404 and BEL7404-CP20 were grown in 96-well plates overnight in DMEM-high glucose medium. Cells were then incubated with various concentrations of free ethacraplatin, M-EA-Pt or cisplatin at Pt concentrations of 0.5, 5, 20, 40, 80, 120, 160 and 200 μM for 48 h. Next, the cells were incubated for 3 h with 100 μL of 3-(4,5-dimethylthiazol-2-yl)-2,5-diphenyltetrazolium bromide (MTT) (final concentration 0.5 mg/mL). Finally, the medium was substituted with 100 μL of DMSO. The absorbance at 570 nm was measured with a microplate reader (Tecan, Durham, USA). All experiments were performed in triplicate.

2.12. *In vivo* antitumor activity

Female NOD SCID mice (18-20 g) were bought from Beijing Vital River Laboratories. All care and handling of animals was performed with the approval of the Animal Ethics Committee of the Medical School, Peking University (Beijing, China). Cisplatin resistant BEL7404-CP20 liver cancer cells were suspended in 100 μL of PBS and Matrigel (Corning, USA) at a 1:1 ratio (v/v), then 10^7 cells were subcutaneously injected into the right flanks of NOD SCID mice. When the tumor volume reached 50-100 mm^3 , five independent *in vivo* antitumor activity experiments with $n = 6$ mice per group were carried out. Cisplatin, free EA-Pt or M-EA-Pt was administered at a Pt dosage of 1.3 mg/kg by tail vein injection. The groups treated

with saline and empty micelles were regarded as controls. M-EA-Pt was synthesized freshly, and the platinum content was determined before every injection. Tumors were measured in two dimensions twice every week and the total volume was calculated using the following formula: tumor volume = $\frac{\text{length} \times \text{width}^2}{2}$. The body weights of the mice were determined every other day to monitor potential side effects.

2.13. Hemolysis experiment

Fresh blood was collected from healthy female NOD SCID mice by retro-orbital bleeds. Red blood cells (RBCs) were isolated from 0.8 mL fresh blood by centrifuging at 10,000g for 5 min. The RBCs were repeatedly rinsed with saline until no color was observed in the supernatant. RBCs were then suspended in 15 mL saline. RBC suspension (0.5 mL) was mixed with 0.5 mL of saline containing different concentrations of M-EA-Pt at 25, 50, 75, 100 and 200 $\mu\text{g}/\text{mL}$ to give final concentrations of 12.5, 25, 37.5, 50 and 100 $\mu\text{g}/\text{mL}$, respectively. The negative control was 0.5 mL RBC suspension mixed with 0.50 mL saline and the positive control was 0.5 mL RBC suspension mixed with 0.50 mL distilled water. The samples were mixed gently, kept at room temperature for 2 h, and then centrifuged at 10,000g for 5 min. The absorbance of the supernatant at 540 nm was recorded in the 96-well plate. The percentage of hemolysis was evaluated as follows:

$$\text{Hemolysis \%} = \frac{\text{Abs}_{\text{sample}} - \text{Abs}_{\text{negative control}}}{\text{Abs}_{\text{positive control}} - \text{Abs}_{\text{negative control}}} \times 100\%$$

2.14. Histological study and blood biochemical analysis

After completion of the *in vivo* antitumor activity experiment, blood was collected by retro-orbital bleeds and centrifuged at 5000 *g* for 10 min. The blood sera were then transferred into several new tubes. The blood serum samples were analyzed for renal function markers (blood urea nitrogen (BUN) and creatinine (Cr)) in the Beijing Lawke Health Laboratory Center for Clinical Laboratory Development.

After the blood was collected, all the mice were euthanized, and the primary organs were excised and fixed in 10% formalin solution. The organ samples were then analyzed in the Beijing Lawke Health Laboratory Center for Clinical Laboratory Development by hematoxylin and eosin (H&E) staining. The stained slides were observed by light microscopy (EVOS XL Core, Thermo Fisher, USA).

2.15. Intratumoral microdistribution of platinum

1×10^7 cisplatin-resistant BEL7404-CP20 liver cancer cells were subcutaneously inoculated into the right flanks of female NOD SCID mice. After the tumor volume reached around 150 mm³, the mice were randomly divided into four group ($n = 3$). Cisplatin, free ethacraplatin or M-EA-Pt was injected intravenously into mice at a Pt dosage of 10 μ mol/kg. The mice, which were used as controls, were intravenously injected with saline. After 24 h, all the mice were euthanized and the tumors were excised and digested in aqua regia at 300 °C. Finally, the platinum content in the tumors was determined by ICP-MS.

3. Results and discussion

3.1. Synthesis and characterization of micelles encapsulating ethacraplatin

Ethacraplatin was synthesized according to the procedures reported previously [10]. The chemical structure and purity of ethacraplatin was verified by its ESI-MS, ^1H NMR, UV-vis and HPLC spectra (Fig. S1-S4). Ethacraplatin was encapsulated within DSPE-PEG₂₀₀₀ micelles by a film dispersion method (Fig. 1A). DSPE forms the hydrophobic core inside the micelle that creates a suitable environment for encapsulating ethacraplatin, while the role of PEG is to provide the hydrophilic ends on the surface that improve the water solubility of the whole drug-loaded micelle. In addition, the circulation time of micelles can also be increased because of the hydrophilic PEG ends, which provide steric stabilization and stealth properties.

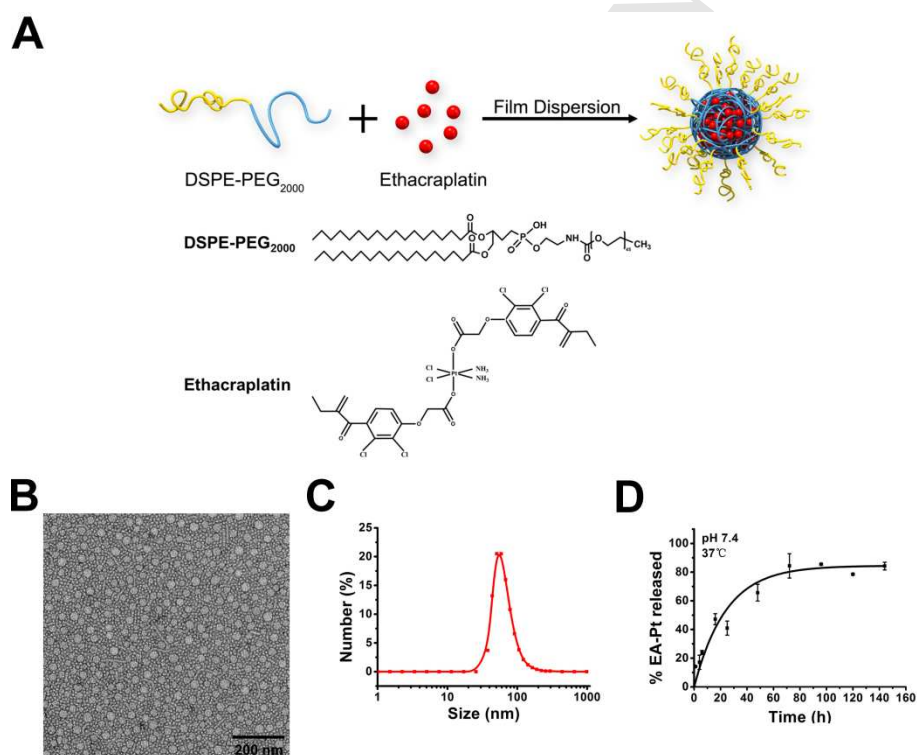


Fig. 1. Characterization of micelles encapsulating ethacraplatin (M-EA-Pt). (A) Schematic illustration of M-EA-Pt. (B) TEM image of M-EA-Pt after staining with 1% uranyl acetate. (C) Size distribution of M-EA-Pt. (D) Release profiles of ethacraplatin from micelles at pH 7.4 and 37 °C. Released platinum was quantified using ICP-MS. Scale bar = 200 nm.

Micelles were prepared using different weight ratios of ethacraplatin (EA-Pt) to DSPE-PEG₂₀₀₀ ($m_{\text{EA-Pt}} : m_{\text{DSPE-PEG2000}}$) (Table S1). The resulting micelles were evaluated for their average hydrodynamic diameters, polydispersity indices (PDI), encapsulation efficiencies and drug loading efficiencies, which were calculated according to the Pt content as quantified by ICP-MS. When the $m_{\text{EA-Pt}} : m_{\text{DSPE-PEG2000}}$ ratio decreased, the diameter of the micelles became smaller, while the encapsulation efficiency increased. We found that it was difficult for our system to form micelles when $m_{\text{EA-Pt}} : m_{\text{DSPE-PEG2000}}$ was smaller than 1:7. Micelles with $m_{\text{EA-Pt}} : m_{\text{DSPE-PEG2000}} = 1:7$ were used in the following study because they had the highest encapsulation efficiency together with an ideal drug loading capacity and PDI (Table S1). According to previous reports [26-28], the resulting particles are of an appropriate size to target passively tumor tissue through the EPR effect.

The morphologies of ethacraplatin-loaded micelles (M-EA-Pt) were examined by TEM. M-EA-Pt micelles were uniform spheres, with a diameter of approximately 40 nm (Fig. 1B). The particle diameters determined by TEM are smaller than the hydrodynamic diameters determined by DLS, due to stretching of the hydrophilic PEG ends and swelling of the micelle cores in aqueous medium (Fig. 1C).

3.2. Controlled release of ethacraplatin *in vitro*

Next, the release profile of ethacraplatin from micelles was evaluated. Aliquots of M-EA-Pt micelles were dialyzed against phosphate buffered saline (PBS) at pH 7.4 and 37 °C. The released platinum content was quantified using ICP-MS. The percentage of encapsulated platinum released over time is presented in Fig. 1D. There

is no obvious burst release, a drawback of micelle-based delivery system, as only 14% of the total platinum was released in the first 1 hour. After 72 hours of incubation, approximately 85% of the total platinum was released (Fig. 1D). The data demonstrated that these M-EA-Pt micelles are an optimal platform for sustained release of platinum.

3.3. Inhibition of the activity of GSTs *in vitro*

To begin with, immunofluorescence was used to confirm the expression of GST- π (a member of the GST family), which was significantly related with the cisplatin resistance of tumor, in the hepatocellular carcinoma cell line BEL7404 and its cisplatin-resistant derivative BEL7404-CP20 (Fig. 2A). GST- π was expressed at much higher levels in the BEL7404-CP20 cells than in the parental cells. This was also confirmed by Western Blot (Fig. 2B). Next, the activity of GSTs in BEL7404 and BEL7404-CP20 cells was verified. The data demonstrated that the activity of GSTs in BEL7404-CP20 was at a significantly higher level (Fig. 2C). These results are consistent with previous reports that GSTs, especially GST- π , contribute to the cisplatin resistance [3-6].

Thereafter, the residual GST activity was determined in BEL7404-CP20 cells after incubation with 50 μ M cisplatin, free EA-Pt or M-EA-Pt for 4 h (Fig. 2D). After incubation, marked inhibition of GST activity was observed in the cells incubated with free EA-Pt and M-EA-Pt. The GST activity in the cells incubated with cisplatin was only slightly lower than that in control group (Fig. 2D). This result indicated that free ethacraplatin and ethacraplatin-encapsulated micelles were able to enter live

mammalian cells and significantly inhibit the GST activity. The activity of GSTs in the BEL7404-CP20 cancer cells incubated with M-EA-Pt was significantly lower than in the cells incubated with free EA-Pt. This might benefit from the higher uptake of M-EA-Pt by cells, which was due to endocytosis of nanomicelles, and the resultant higher GSTs inhibition than free EA-Pt. These results indicated that M-EA-Pt had stronger ability than free EA-Pt in GSTs inhibition.

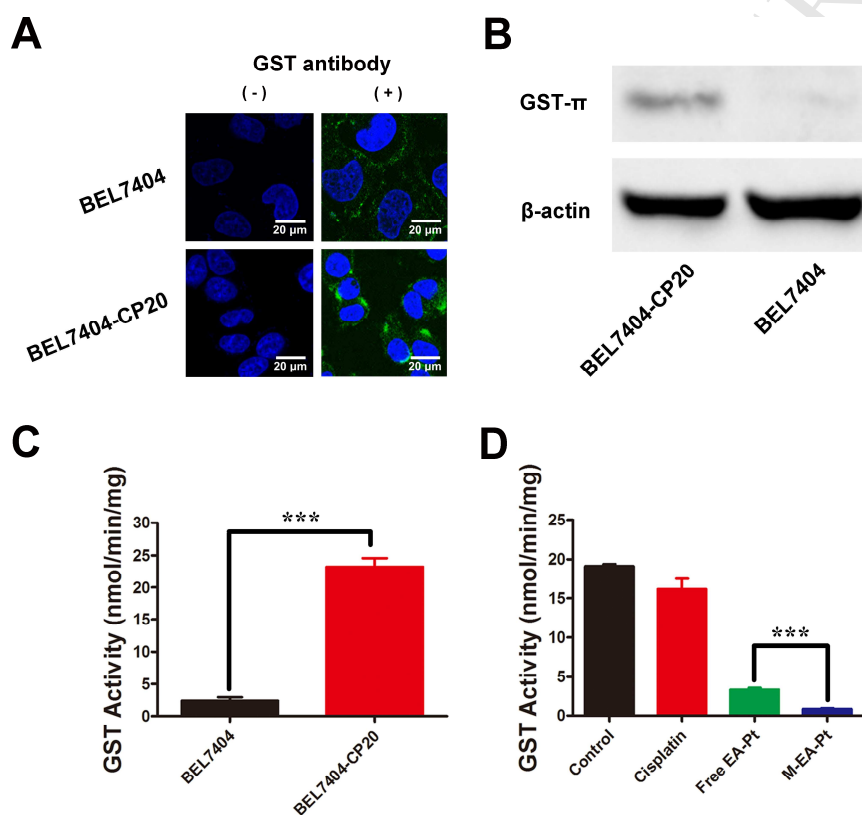


Fig. 2. GST- π expression and GST activity in cells. (A) Detection of GST- π expression (green) in BEL7404 and BEL7404-CP20 cells by confocal fluorescence microscopy. Cells were pretreated with (+) or without (-) a primary monoclonal GST antibody, then incubated with goat anti-mouse secondary antibody conjugate with FITC (green). Nuclei are stained with DAPI (blue). (B) Western blot analysis of GST- π in BEL7404 and BEL7404-CP20 cells. β -actin represented a protein-loading control. (C) Activity of GSTs in BEL7404 and BEL7404-CP20 cells. (D) Residual

GST activity of BEL7404-CP20 cells after exposure to cisplatin, free EA-Pt or M-EA-Pt at Pt concentrations of 50 μM . The control group was untreated cells. Data are presented as means \pm SD ($n = 3$), *** $P < 0.001$.

3.4. Anti-cancer efficacy *in vitro*

The anti-cancer efficacy of M-EA-Pt was evaluated in BEL7404 and BEL7404-CP20 cells. The two cancer cell lines were incubated with cisplatin, free EA-Pt and M-EA-Pt at different platinum concentrations for 48 h and the cell viability was assessed by MTT assay. For the cisplatin-sensitive cancer cells, the anticancer efficacy of cisplatin is superior to free ethacraplatin and M-EA-Pt (Fig. S5). For the cisplatin-resistant cancer cells, free ethacraplatin and M-EA-Pt outperformed cisplatin (Fig. 3A). For both EA-Pt and M-EA-Pt, the resistance factors (RF) are approximately 1, which means that the cisplatin resistance is almost overcome (Table 1). Furthermore, IC_{50} of M-EA-Pt (33.0 μM) was lower than that of free ethacraplatin (58.9 μM) in resistant cells and this phenomenon was also observed in the cisplatin-sensitive cancer cells. The empty micelles formed by DSPE-PEG₂₀₀₀ showed ignorable cytotoxicity toward BEL7404 and BEL7404-CP20 cells (Fig. S6). These results highlighted that micelle formation enhanced the anticancer efficacy of ethacraplatin in cancer cells, especially in cisplatin-resistant cells.

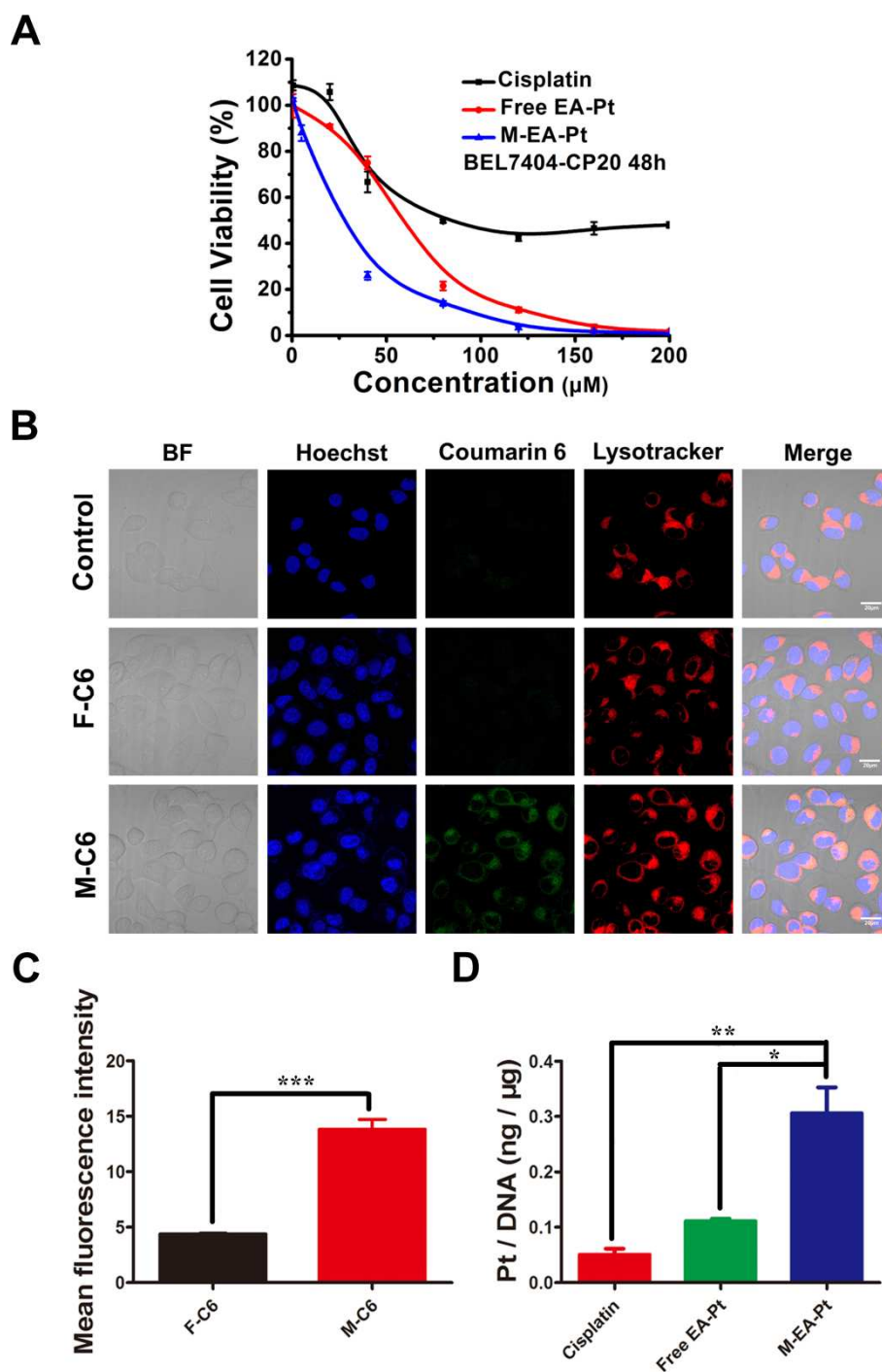


Fig. 3. Evaluation of *in vitro* antitumor activity. (A) *In vitro* antitumor activity of cisplatin, free EA-Pt and M-EA-Pt toward BEL7404-CP20 cells. (B) BEL7404-CP20 cells were incubated with F-C6 and M-C6, then the cellular internalization and distribution of C6 were imaged by confocal fluorescence microscopy. The control group was untreated cells. DNA is labeled by Hoechst (blue). Endosomes/lysosomes are labeled by Lystotracker (red). (C) Statistical analysis of the

mean fluorescence intensity of C6 from the confocal fluorescence microscopy data. (D) Platinum content in the genomic DNA of BEL7404-CP20 cells after incubation with cisplatin, free EA-Pt or M-EA-Pt at a Pt concentration of 50 μM for 4 h. Data are presented as means \pm SD ($n = 3$), * $P < 0.05$, ** $P < 0.01$, *** $P < 0.001$. Scale bar = 20 μm .

Table 1. Comparison of IC_{50} and drug-resistance factor of cisplatin, free EA-Pt, M-EA-Pt and empty micelles in BEL7404 and BEL7404-CP20 cells. Data are presented as means \pm SD ($n = 3$).

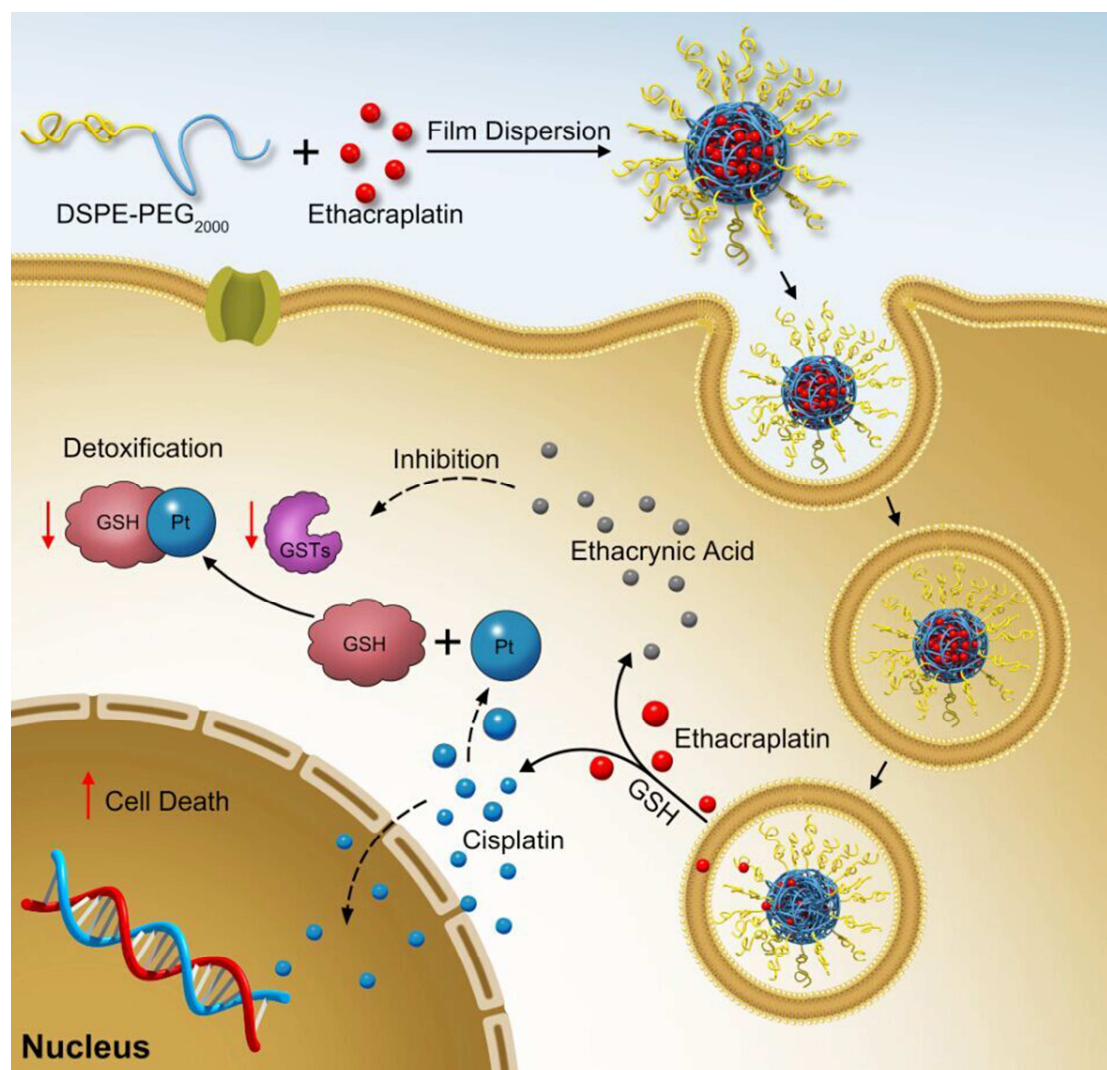
Test Compound	IC_{50} (μM)		Resistance Factor (RF)
	BEL7404	BEL7404-CP20	
Cisplatin	12.2 \pm 0.9	76.4 \pm 2.4	6.26
EA-Pt	55.0 \pm 0.8	58.9 \pm 0.5	1.08
M-EA-Pt	28.9 \pm 0.5	33.0 \pm 0.5	1.14
Empty Micelles	> 200	114	-

In sensitive cancer cell lines, cisplatin is more active than EA-Pt and M-EA-Pt. This is due to the following two reasons. 1. Since GSTs are not highly expressed in sensitive cell lines, cisplatin can exert its activity normally, while the GSTs inhibition ability of EA-Pt and M-EA-Pt don't contribute to a higher level of active platinum in nuclei. 2. On the other hand, the cytotoxicity of EA-Pt and M-EA-Pt are slightly limited by the rate and efficiency of their transformation in cells to cisplatin. However, in resistant cancer cell lines, EA-Pt and M-EA-Pt outperformed cisplatin. The highly expressed GSTs in resistant cell lines would accelerate the deactivation of cisplatin, but they have much less effect on EA-Pt and M-EA-Pt that have ability of GSTs inhibition. Although the process of their transformation to active species in cells

slightly decreased the efficiency of EA-Pt and M-EA-Pt, the circumvention of EA-Pt and M-EA-Pt from inactivation by GSTs/GSH pathway endowed them with higher cytotoxicity than cisplatin in resistant cell lines.

3.5. Internalization and distribution of micelles *in vitro*

The internalization of micelles was investigated at the subcellular level using confocal laser scanning microscopy (CLSM). As ethacraplatin does not possess fluorescent properties, a fluorescent molecule coumarin 6 (C6) was encapsulated within the DSPE-PEG₂₀₀₀ micelles for the observation of micelle behavior in cells. Thereafter, BEL7404 and BEL7404-CP20 cells were incubated with free C6 (F-C6) and C6-loaded micelles (M-C6). After 30 min, stronger green fluorescence from C6 was observed in the cells incubated with M-C6 than in the cells treated with F-C6 (Fig. 3B-C, Fig. S7). This result clearly indicated that M-C6 was more rapidly and effectively internalized than F-C6 into the cancer cells. Micelle formation significantly increased the intracellular C6 accumulation in both cisplatin-resistant and parental cancer cells. Furthermore, most of the fluorescent signals from M-C6 were co-localized with endosomes/lysosomes labeled by the LysoTracker Deep Red marker, suggesting that internalization of the micelles was related to endocytic pathways [29]. Consequently, we conclude that micelle formation is capable of enhancing the GST inhibitory activity and the anticancer efficacy of ethacraplatin by increasing drug uptake by cancer cells, especially by cisplatin-resistant cancer cells (Scheme 1).



Scheme 1. Scheme of release of EA-Pt in cisplatin-resistant cells after endocytosis of M-EA-Pt.

The diagram shows the mechanism by which ethacrynic acid (EA) inhibits glutathione S-transferases (GSTs) to circumvent the cisplatin resistance of cancer cells.

3.6. Quantification of platinum-DNA adduct formation

It is generally known that cell death caused by cisplatin mainly derives from formation of platinum-DNA adducts. To quantify and compare the content of platinum-DNA adducts, we exposed BEL7404-CP20 cancer cells to 50 μ M cisplatin, free EA-Pt or M-EA-Pt for 4 h. The genomic DNA was isolated using a DNA miniprep kit. The formation of platinum-DNA adducts was determined by quantifying

the Pt content in the genomic DNA by ICP-MS. Compared with cells treated with cisplatin, the DNA from cells treated with both free EA-Pt and M-EA-Pt exhibited significantly higher levels of platinum-DNA adducts (Fig. 3D). These data suggested that, comparing with cisplatin, free EA-Pt and M-EA-Pt have more active platinum species to enter into nuclei, which owed to their GSTs inhibition ability. Moreover, cells treated with M-EA-Pt contained 2.76 times more platinum-DNA adducts than that treated with free EA-Pt, which corroborated our hypothesis that the M-EA-Pt formulation might be capable of enhancing the antitumor activity of EA-Pt in the cisplatin-resistant cancer cells due to a higher level of DNA damage. This is consistent with the higher internalization of M-C6 in cells.

3.7. Anti-cancer efficacy *in vivo*

As M-EA-Pt showed promising results in cisplatin-resistant cancer cells in the *in vitro* experiment, we next tested the anticancer efficacy *in vivo*. First of all, the excellent blood compatibility of M-EA-Pt was verified (Fig. S8). After that, we assessed the anticancer efficacy of M-EA-Pt in the cisplatin-resistant BEL7404-CP20 human liver cancer subcutaneous mouse model. BEL7404-CP20 tumor-bearing mice were treated by intravenous injections of saline, empty micelles, cisplatin, free EA-Pt and M-EA-Pt (platinum dose of 1.3 mg/kg) every 3 days. When the tumor growth was monitored for 30 days, no obvious inhibition of tumor growth was observed in the mice treated with cisplatin or free EA-Pt compared with the control groups (mice treated with saline and empty micelles) (Fig. 4A). However, M-EA-Pt significantly repressed tumor growth compared to the controls. The antitumor efficiency was

further confirmed by histological analysis of tumor tissues using the hematoxylin and eosin (H&E) staining method. A number of vacuoles in cytoplasm and obvious cell shrinkage and nuclear condensation were only observed in the M-EA-Pt-treated group, while the other groups did not exhibit these changes in the tumor tissue, which indicated M-EA-Pt can induce high level of apoptosis *in vivo* (Fig. 4E). This result strongly supported our hypothesis that M-EA-Pt overcame cisplatin resistance, thereby achieving enhanced anticancer efficacy. Moreover, no significant loss of body weight was observed in the M-EA-Pt treatment group, compared with the 10% body weight loss in the cisplatin group (Fig. 4B). In addition, only two mice survived in the cisplatin-treated group at the end of the treatment, once again indicating that cisplatin exhibits fatal side effects (Fig. 4C). These results suggested that M-EA-Pt overcomes cisplatin-resistance of tumor, circumvents possible side effects associated with cisplatin and exhibit significantly enhanced inhibition efficiency against cisplatin-resistant tumor over cisplatin and free EA-Pt.

Cisplatin is obviously powerless to treat cisplatin-resistant cancers, since the highly expressed GSTs in cisplatin-resistant cancers would partly deactivate cisplatin and decrease the effective platinum content in nuclei. Free EA-Pt shows antitumor activity and overcomes drug resistance in the *in vitro* assay, but is not effective enough to fight resistant cancer cells *in vivo* as water solubility is critical for drug availability after injection. These phenomena emphasize the fact that GSTs inhibition and micelle formation are crucially important to achieve the antitumor activity of M-EA-Pt micelles in the treatment of cisplatin-resistant cancers.

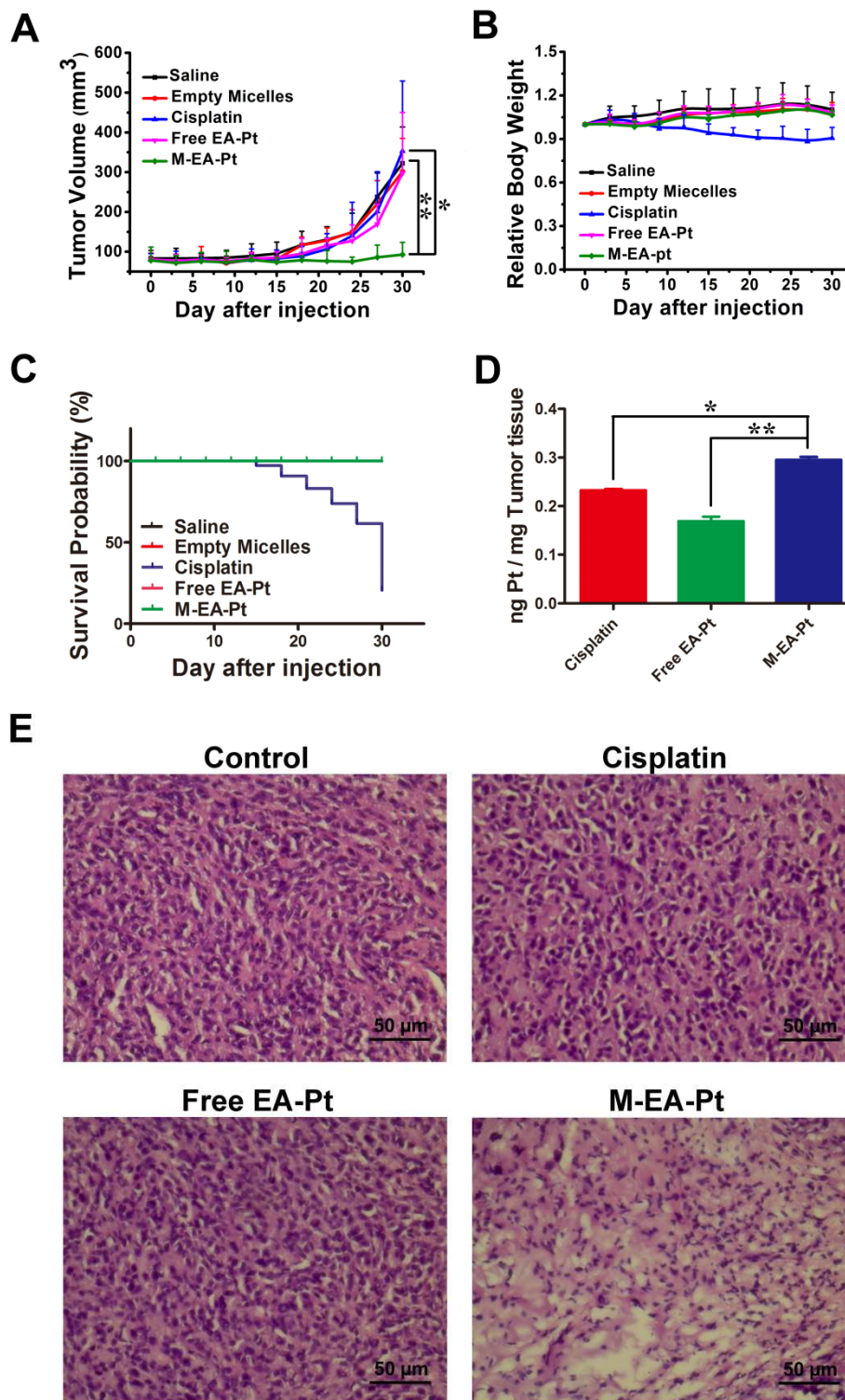
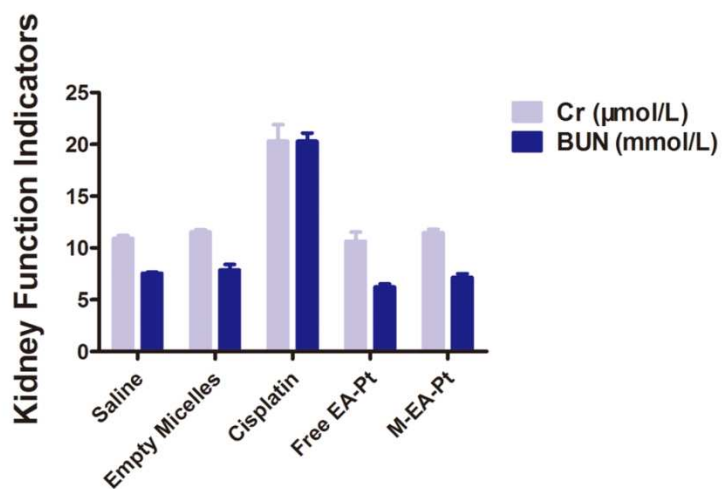


Fig. 4. *In vivo* antitumor efficacy study. (A) *In vivo* tumor growth inhibition curves of BEL7404-CP20 tumor-bearing mice treated with saline, empty micelles, cisplatin, free EA-Pt or M-EA-Pt twice a week for 4 weeks. Data are presented as means \pm SD ($n = 6$). (B) Relative body weight of BEL7404-CP20 tumor-bearing mice treated with saline, empty micelles, cisplatin, free EA-Pt or

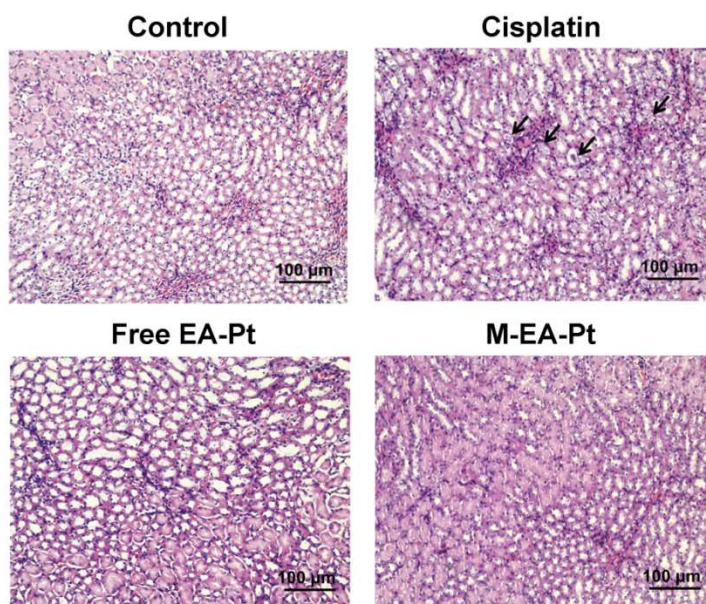
M-EA-Pt over the course of the treatment. Data are presented as means \pm SD ($n = 6$). (C) Survival curve of BEL7404-CP20 tumor-bearing mice over the course of the treatment. Data are presented as means \pm SD ($n = 6$). (D) Intratumoral microdistribution of platinum in BEL7404-CP20 tumor tissues, as measured by ICP-MS, 24 h post-administration of cisplatin, free EA-Pt or M-EA-Pt. Data are presented as means \pm SD ($n = 3$). (E) Histological study of BEL7404-CP20 tumor tissues. * $P < 0.05$, ** $P < 0.01$. Scale bar = 50 μ m.

Next, the toxicity of the different treatments was further ascertained by histological study and blood biochemistry analysis. After completion of the study, histological analysis of sections of heart, liver, spleen, lung and kidney was performed by the H&E staining method. The blood of mice in all the treatment groups was collected to assess the levels of creatinine (Cr) and blood urea nitrogen (BUN). Marked changes were only observed in the cisplatin-treated group (Fig. 5A). Histological staining revealed that cisplatin administration caused hyaline cast filling in the renal tubules, which indicated renal failure (Fig. 5B-C). Meanwhile, These data are consistent with a previous report that nephrotoxicity is the dose-limiting toxicity of cisplatin [30]. No apparent nephrotoxicity was detected in the other treated groups. Overall, the above-mentioned results demonstrated that our system is an outstanding candidate with high efficiency and low toxicity for chemotherapy of cisplatin-resistant cancer.

A



B



C

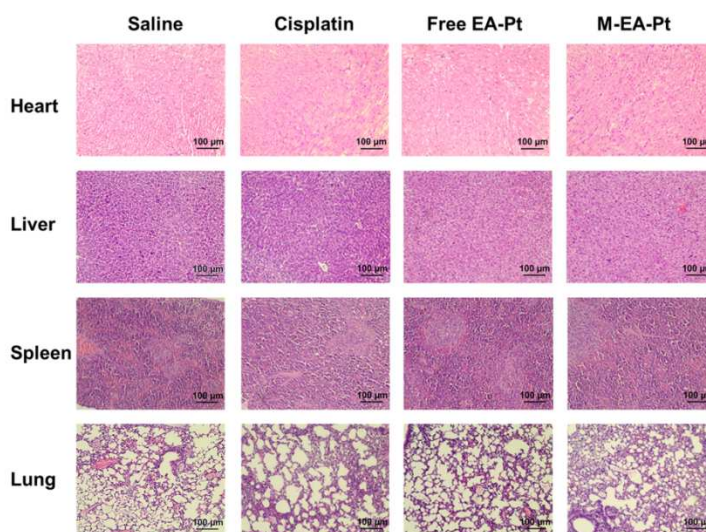


Fig. 5. *In vivo* toxicity of cisplatin, free EA-Pt and M-EA-Pt. (A) Blood analysis of urea nitrogen (BUN) and creatinine (Cr) at completion of the treatment with cisplatin, free EA-Pt or M-EA-Pt. Saline was administered as a control. (B) Histological study of kidney sections at completion of the treatment with cisplatin, free EA-Pt or M-EA-Pt. Saline was administered as a control. Black arrows indicate hyaline cast filling in the renal tubules. (C) Histological study of heart, liver, spleen and lung of BEL7404-CP20 tumor-bearing mice at completion of the treatment with cisplatin, free EA-Pt or M-EA-Pt. Saline was administered as a control. Data are presented as means \pm SD ($n = 3$). Scale bar = 100 μ m.

Finally, the intratumoral microdistribution of platinum in BEL7404-CP20 tumor tissues was investigated (Fig. 4D). The data demonstrated that the level of Pt in the tumor tissue was much higher in the M-EA-Pt-treated mice than in the mice treated with free EA-Pt. This may be because the EPR effect promotes the accumulation of nanosized micelles. The higher accumulation of platinum in the tumor contributed to the improved antitumor activities of M-EA-Pt.

4. Conclusion

In summary, we encapsulated a GST inhibitor axial-conjugated Pt(IV) prodrug, named ethacraplatin, into the DSPE-PEG₂₀₀₀ micelles for treatment of cisplatin-resistant cancer. The obtained ethacraplatin-loaded micelles have uniform size, high monodispersity and controlled release properties. The micelles were able to inhibit GST activity in cancer cells more strongly than the free drug. Our data proved that unlike the free drug, this developed M-EA-Pt system has the potency to tackle cisplatin resistance and inhibit cisplatin-resistant tumor growth *in vitro* and *in vivo*.

Furthermore, the micelles circumvented the nephrotoxicity of cisplatin and exhibited very low system toxicity. These results provide strong evidence that GSTs inhibitor-modified cisplatin prodrug combined with nanoparticle encapsulation favor high effective platinum accumulation, significantly enhanced antitumor efficacy against cisplatin-resistant cancer and decreased systemic toxicity. We believe that these ethacraplatin-loaded micelles, with their excellent *in vivo* efficacy and low toxicity, will improve the prospects for chemotherapy of cisplatin-resistant cancers in the near future.

Author contribution

S.L., C.L. and X.-J.L. designed research; S.L., C.L., S.J., J.L., X.X., A.S.E., J.S., J.T. and J.D. performed research; S.L., C.L., and X.-J.L. analyzed data; and S.L. and C.L. wrote the paper.

Notes

The authors declare no conflict of interest.

Appendix A. Supplementary data

Characterization of ethacraplatin, ethacraplatin-loaded nanomicelles, cytotoxicity of empty micelles and blood compatibility of M-EA-Pt are described in *SI Appendix*.

Acknowledgements

This work was supported by the Beijing Natural Science Foundation [grant No. 7174332]; National Natural Science Foundation of China [grant No. 31600810]; Natural Science Foundation key project [grant No. 31630027, 31430031]; and the National Distinguished Young Scholars grant [grant No. 31225009]. The authors also

appreciate support by the Strategic Priority Research Program of the Chinese Academy of Sciences [grant No. XDA09030301] and the external cooperation program of BIC, Chinese Academy of Science [grant No. 121D11KY5B20130006].

Reference

- [1] L.A. Torre, F. Bray, R.L. Siegel, J. Ferlay, J. Lortet - Tieulent, A. Jemal, Global cancer statistics, 2012, *CA-Cancer J. Clin.* 65 (2015) 87-108.
- [2] D.-W. Shen, L.M. Pouliot, M.D. Hall, M.M. Gottesman, Cisplatin resistance: a cellular self-defense mechanism resulting from multiple epigenetic and genetic changes, *Pharmacol. Rev.* 64 (2012) 706-721.
- [3] D.M. Townsend, K.D. Tew, The role of glutathione-S-transferase in anti-cancer drug resistance, *Oncogene* 22 (2003) 7369-7375.
- [4] S. Goto, T. Iida, S. Cho, M. Oka, S. Kohno, T. Kondo, Overexpression of glutathione S-transferase π enhances the adduct formation of cisplatin with glutathione in human cancer cells, *Free Radical Res.* 31 (1999) 549-558.
- [5] M. Pasello, F. Michelacci, I. Scionti, C.M. Hattinger, M. Zuntini, A.M. Caccuri, K. Scotlandi, P. Picci, M. Serra, Overcoming glutathione S-transferase P1-related cisplatin resistance in osteosarcoma, *Cancer Res.* 68 (2008) 6661-6668.
- [6] M. Schultz, S. Dutta, K.D. Tew, Inhibitors of glutathione S-transferases as therapeutic agents, *Adv. Drug Deliver. Rev.* 26 (1997) 91-104.
- [7] S. Dhar, S.J. Lippard, Mitaplatin, a potent fusion of cisplatin and the orphan drug dichloroacetate, *Proc. Nat. Acad. Sci. USA* 106 (2009) 22199-22204.
- [8] K. Suntharalingam, Y. Song, S.J. Lippard, Conjugation of vitamin E analog α -TOS to Pt (IV) complexes for dual-targeting anticancer therapy, *Chem. Commun.* 50 (2014) 2465-2468.
- [9] X. Xue, S. You, Q. Zhang, Y. Wu, G.Z. Zou, P.C. Wang, Y.L. Zhao, Y. Xu, L. Jia, X. Zhang, Mitaplatin increases sensitivity of tumor cells to cisplatin by inducing mitochondrial dysfunction, *Mol. Pharm.* 9 (2012) 634-644.
- [10] W.H. Ang, I. Khalaila, C.S. Allardyce, L. Juillerat-Jeanneret, P.J. Dyson, Rational design of platinum (IV) compounds to overcome glutathione-S-transferase mediated drug resistance, *J. Am.*

Chem. Soc. 127 (2005) 1382-1383.

[11] K. Ajima, T. Murakami, Y. Mizoguchi, K. Tsuchida, T. Ichihashi, S. Iijima, M. Yudasaka, Enhancement of in vivo anticancer effects of cisplatin by incorporation inside single-wall carbon nanohorns, *ACS Nano* 2 (2008) 2057-2064.

[12] S. Dhar, N. Kolishetti, S.J. Lippard, O.C. Farokhzad, Targeted delivery of a cisplatin prodrug for safer and more effective prostate cancer therapy in vivo, *Proc. Nat. Acad. Sci. USA* 108 (2011) 1850-1855.

[13] N. Graf, D.R. Bielenberg, N. Kolishetti, C. Muus, J. Banyard, O.C. Farokhzad, S.J. Lippard, $\alpha V\beta 3$ integrin-targeted PLGA-PEG nanoparticles for enhanced anti-tumor efficacy of a Pt (IV) prodrug, *ACS Nano* 6 (2012) 4530-4539.

[14] T.C. Johnstone, K. Suntharalingam, S.J. Lippard, The Next Generation of Platinum Drugs: Targeted Pt (II) Agents, Nanoparticle Delivery, and Pt (IV) Prodrugs, *Chem. Rev.* 116 (2016) 3436-3486.

[15] S. Marrache, R.K. Pathak, S. Dhar, Detouring of cisplatin to access mitochondrial genome for overcoming resistance, *Proc. Nat. Acad. Sci. USA* 111 (2014) 10444-10449.

[16] D.P. Nowotnik, E. Cvitkovic, ProLindac™(AP5346): a review of the development of an HPMA DACH platinum polymer therapeutic, *Adv. Drug Deliver. Rev.* 61 (2009) 1214-1219.

[17] H. Xiao, R. Qi, S. Liu, X. Hu, T. Duan, Y. Zheng, Y. Huang, X. Jing, Biodegradable polymer-cisplatin (IV) conjugate as a pro-drug of cisplatin (II), *Biomaterials* 32 (2011) 7732-7739.

[18] H. Xiao, L. Yan, Y. Zhang, R. Qi, W. Li, R. Wang, S. Liu, Y. Huang, Y. Li, X. Jing, A dual-targeting hybrid platinum (IV) prodrug for enhancing efficacy, *Chem. Commun.* 48 (2012) 10730-10732.

[19] H. Xiao, D. Zhou, S. Liu, Y. Zheng, Y. Huang, X. Jing, A complex of cyclohexane-1, 2-diaminoplatinum with an amphiphilic biodegradable polymer with pendant carboxyl groups, *Acta. Biomater.* 8 (2012) 1859-1868.

[20] J. Yang, X. Sun, W. Mao, M. Sui, J. Tang, Y. Shen, Conjugate of Pt (IV)-histone deacetylase inhibitor as a prodrug for cancer chemotherapy, *Mol. Pharm.* 9 (2012) 2793-2800.

[21] T.C. Johnstone, N. Kulak, E.M. Pridgen, O.C. Farokhzad, R. Langer, S.J. Lippard, Nanoparticle encapsulation of mitaplatin and the effect thereof on in vivo properties, *ACS Nano* 7 (2013) 5675-5683.

[22] D. Liu, C. Poon, K. Lu, C. He, W. Lin, Self-assembled nanoscale coordination polymers with

- trigger release properties for effective anticancer therapy, *Nat. Commun.* 5 (2014) 1-11.
- [23] J. Kim, S. Pramanick, D. Lee, H. Park, W.J. Kim, Polymeric biomaterials for the delivery of platinum-based anticancer drugs, *Biomater. Sci.* 3 (2015) 1002-1017.
- [24] Y. Wang, P. Liu, L. Qiu, Y. Sun, M. Zhu, L. Gu, W. Di, Y. Duan, Toxicity and therapy of cisplatin-loaded EGF modified mPEG-PLGA-PLL nanoparticles for SKOV3 cancer in mice, *Biomaterials* 34 (2013) 4068-4077.
- [25] H. Unterweger, R. Tietze, C. Janko, J. Zaloga, S. Lyer, S. Dürr, N. Taccardi, O.-M. Goudouri, A. Hoppe, D. Eberbeck, Development and characterization of magnetic iron oxide nanoparticles with a cisplatin-bearing polymer coating for targeted drug delivery, *Int. J. Nanomed.* 9 (2014) 3659.
- [26] T.M. Allen, P.R. Cullis, *Drug Delivery Systems: Entering the Mainstream*, *Science* 303 (2004) 1818-1822.
- [27] S. Ganta, H. Devalapally, A. Shahiwala, M. Amiji, A review of stimuli-responsive nanocarriers for drug and gene delivery, *J. Control. Release* 126 (2008) 187-204.
- [28] T. Patel, J. Zhou, J.M. Piepmeier, W.M. Saltzman, Polymeric nanoparticles for drug delivery to the central nervous system, *Adv. Drug Deliver. Rev.* 64 (2012) 701-705.
- [29] X. Duan, D. Liu, C. Chan, W. Lin, Polymeric Micelle - Mediated Delivery of DNA - Targeting Organometallic Complexes for Resistant Ovarian Cancer Treatment, *Small* 11 (2015) 3962-3972.
- [30] S. Dasari, P.B. Tchounwou, Cisplatin in cancer therapy: molecular mechanisms of action, *Eur. J. Pharmacol.* 740 (2014) 364-378.

TOC

